Strain Hardening in Highly Acetylated Chitosan Gels

Franco Furlani,[#] Andrea Marfoglia,[#] Eleonora Marsich, Ivan Donati, and Pasquale Sacco*

ABSTRACT: Strain hardening has recently emerged as a near-universal response of biological tissues to mechanical stimulation as well as a powerful regulator of cell fate. Understanding the mechanistic basis for this nonlinear elasticity is crucial for developing bioinspired materials that mimic extracellular matrix mechanics. Here, we show that covalent networks built from highly acetylated chitosans exhibit strain hardening at physiological pH and osmolarity. While varying the chitosan physical−chemical composition and network connectivity, we provide evidence that temporary nodes arising from the entangling of chains between stable cross-links are at the root of nonlinear elasticity. The contour length (L_c) of the said chains revealed that the larger the chain length between the cross-links, the greater is the entanglement over disentanglement upon network stretching. To this end, we calculated that the minimum number of Khun's segments in L_c that contributes to the onset of strain hardening is 15. Furthermore, we identified a relationship between critical strain marking nonlinear elasticity and the network connectivity, being similar to that found for the cytoskeletal collagen matrix, indicating the potential use of semiflexible (neutral pH-soluble) chitosans in assembling extracellular matrix mimics.

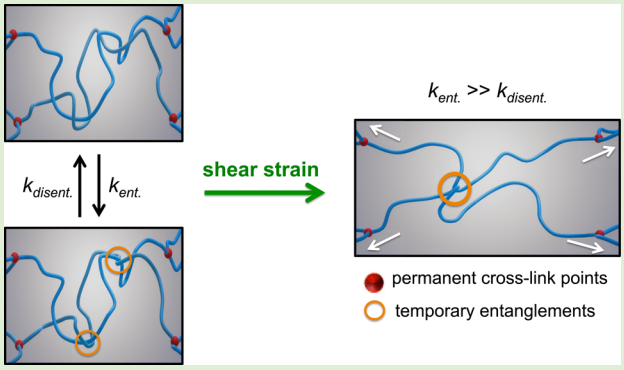

1. INTRODUCTION

Strain hardening, that is, the increase of elastic response under stress or strain, is a nearly universal response of biological tissues to mechanical stimulation. While deforming, all protein-based networks composed of collagen, neurofilaments, fibrin, and actin exhibit nonlinear elasticity.[1] Polysaccharide hydrogels, though less common in nature, can exhibit strain hardening in the same way. Indeed, alginate,[2] agarose,[3] pectin,[4] and methylcellulose[5] in gel state were found to stiffen as shear stress increased. Mechanistically, two major concepts explain such a behavior: (i) polymer chains with low connectivity, that is, cross-linking density well below the central-force isostatic point, can reorganize under shear, forming ordered and more rigid networks prior to fracturing; (ii) while increasing the mechanical stimulation, additional and transient junctions can be formed among polymer chains. Irrespective of the molecular mechanism, strain hardening has emerged a powerful controller of cell fate;[6] thus, mimicking the nonlinear mechanics of natural tissues using polysaccharide hydrogels is now attractive.[7]

The term chitosan refers to a class of binary hetero-polysaccharides composed of β-1 → 4 linked 2-acetamido-2-deoxy-β-D-glucopyranose (*N*-acetyl-glucosamine, A unit) and 2-amino-2-deoxy-β-D-glucopyranose (glucosamine, D unit) residues that occur in varying proportions and patterns along the polymer chain. Chitosans are primarily derived from chitin, a structural component of the exoskeleton of animals belonging to the phylum *Arthropoda*, although chitin can also be found in the cell walls of certain fungi. Chemically, homogeneous or heterogeneous deacetylation of chitin results in chitosans with varying fractions of acetylated units, or F_A, and a random or more block-wise distribution of the two building sugars.[8,9] Aside from molecular weight, F_A plays an important role in modulating chitosan solubility. While all chitosans are soluble in acidic conditions, medium-to-high molecular weight chitosans require F_A in the range 0.4−0.6 to be soluble at neutral pH.[10]

Over the last years, various research groups have proposed strategies for assembling macroscopic chitosan gels. Domard and colleagues described the physical gelation of chitosan using hydrophobic interactions/hydrogen bonds between polymer chains rather than an external cross-linker. This has been accomplished using aqueous ammonia solutions or hydro-alcoholic media.[11−13] In this context, chitosan has been physically gelled using multivalent anions or oppositely charged oligomers.[14−17] Mechanically, the resulting gels behave, in essence, as viscoelastic materials, meaning that they respond to loading or deformation in a time- and frequency-dependent manner. Physical chitosan gels respond

linearly to increasing strain under oscillatory shear up to a critical deformation where strain softening manifests itself due to the progressive unzipping of junctions.

Covalent reticulation has also been studied for the purpose of developing chitosan gels.[18,19] Unlike physical gelation, covalent reticulation promotes, usually, the assembly of mainly elastic materials, which, in theory, fracture without apparent strain softening. Catechol-modified chitosan gels, for example, demonstrated the latter behavior.[20] On the other hand, a recent contribution reported unexpectedly opposing results. Zhang and colleagues developed PEG-grafted covalent chitosan gels that hardened at neutral pH, physiological osmolarity and T = 37 °C.[21] Similarly, our research group created dual cross-linked gels based on a lactose-modified chitosan, which demonstrated significant nonlinear elasticity in the same experimental conditions due to the presence of transient cross-links, despite the presence of permanent junctions.[22]

Here, we aim to uncover the mechanistic basis of strain hardening observed in covalent chitosan gels assembled at neutral pH and physiological osmolarity. To accomplish this goal, two neutral pH-soluble chitosans with high acetylation degree ($F_A \sim 0.6$) and different molecular weight were prepared *via* heterogeneous deacetylation or homogeneous re-*N*-acetylation processes. Following its ability to bind primary amines of chitosan at neutral pH, genipin, an aglycone extracted from *Gardenia jasminoides*, was chosen as a covalent cross-linker.[23] We show that the formation of shear-induced physical entanglements plays a critical role in eliciting nonlinear elasticity while varying the overall network connectivity. Interestingly, despite the significant difference in chain rigidity, we provide evidence that the current gelling system shares similarities with the biological collagen matrix in terms of shear strain *versus* network connectivity curve profile.[24]

2. MATERIALS AND METHODS

2.1. Materials. Novamatrix/FMC Biopolymer (Sandvika, Norway) kindly provided the high-molecular-weight chitosan (fraction of acetylated units, F_A, 0.14) in a base form ($GlcNH_2$). Chitin from crab shells, phosphate-buffered saline (PBS), D_2O, deuterium chloride (DCl), sodium deuteroxide (NaOD), sodium nitrite ($NaNO_2$), and sodium hydroxide (NaOH) were all purchased from Sigma-Aldrich Chemical Co. The composition of PBS was 137 mM NaCl, 2.7 mM KCl, and 10 mM phosphate buffer, with the final ionic strength (I) of 168 mM and pH 7.4. Genipin was obtained from Challenge Bioproducts Co., Ltd. (Taiwan). All reagents and chemicals were of high purity grade. Deionized water was used in all preparations.

2.2. Synthesis and Characterization of Highly Acetylated Chitosans. High-molecular-weight chitosan (HMWc) with starting F_A = 0.14 was re-*N*-acetylated in hydroalcoholic media using acetic anhydride as the acetyl group donor and converted into its chloride form as previously described.[25] Low-molecular-weight chitosan (LMWc) was produced from chitin by exploiting a two-step low-temperature alkaline swelling/high-temperature heterogeneous deacetylation reaction.[26] Briefly, 2.5 g of chitin flakes (milled in a mortar to particles less than 1 mm) was added to 43 mL of ice-cold 20 M NaOH in a 100 mL glass beaker. Chitin was then allowed to swell at around 10 °C for 3 days under magnetic stirring. The beaker was then transferred in a warm water bath at 60 °C under magnetic stirring for 1 h to promote chitin deacetylation. The resulting dispersion was transferred to a sieve and vacuum-filtered. Then, chitosan was washed extensively by deionized warm water until neutral pH was achieved. Chitosan was gathered, transferred to a glass Petri dish, and dried overnight at T = 37 °C. The dried chitosan was weighed, solubilized at a concentration of 1 g/L using 0.2 M acetic acid as the solvent, and filtered through 1.2 μm filters to remove insoluble aggregates and residual chitin contaminants. To convert chitosan into its hydrochloride form, the solution was then transferred in a dialysis tube (average flat width, 33 mm; cutoff 12,000; Sigma-Aldrich, Chemical Co.) and subjected to successive shifts at T = 8 °C as follows: (i) 1 day in 0.2 M NaCl /32 μM HCl, pH 4.5; (ii) 1 day in 32 μM HCl, pH 4.5; (iii) deionized water until the conductivity was below 3 μS/cm. Finally, the solution was freeze-dried.[27] The yield of the process resulted around 35% w/w.

To determine the molecular weight of chitosans, the intrinsic viscosity of both HMWc and LMWc was measured at T = 25 °C by means of an AVS370 viscosity measuring apparatus, equipped with a CT 72/P thermostat (SI Analytics), using an Ubbelohde-type viscometer. A buffer solution composed of 20 mM AcOH/AcNa, pH 4.5, and 100 mM NaCl was used as the solvent. The intrinsic viscosity values were determined by recording the polymer concentration dependence of the reduced specific viscosity, η_{sp}/c, and of the reduced logarithm of the relative viscosity, $\ln(\eta_{rel})/c$, by using the Huggins (1) and Kraemer (2) equations, respectively

$$\frac{\eta_{sp}}{c} = [\eta] + k[\eta]^2 c \tag{1}$$

$$\frac{\ln \eta_{rel}}{c} = [\eta] - k'[\eta]^2 c \tag{2}$$

where k and k' are the Huggins and Kraemer constants, respectively. The corresponding weight-average molecular mass ($\bar{M}_w$) of both chitosans was calculated according to the Mark–Houwink–Sakurada equation (eq 3)

$$[\eta] = K \cdot \bar{M}_w^{\ a} \tag{3}$$

where parameters K and a were 8.43×10^{-3} mL/g and 0.92, respectively.[28]

F_A was determined by ^{1}H NMR spectroscopy. Chitosan samples were prepared as follows: 20 mg of the polymer was solubilized in 2 mL of deuterium oxide (D_2O) and then 150 μL of deuterium chloride (DCl) was added under vigorous stirring and mild heating. Then, 30 μL of sodium nitrite ($NaNO_2$, 10 mg/mL) was added in D_2O, and the resulting solution was stirred for 2 h. Finally, the pD value was increased to 3–4, and 700 μL of chitosan samples were transferred into NMR tubes and analyzed by means of a 400 VNMRS Varian NMR spectrometer operating at 400 MHz. The spectra were recorded at 85 °C. Table 1 recapitulates the physical–chemical characteristics of the two chitosans used in this study.

Table 1. Physical–Chemical Parameters of Chitosans Used in This Study[a]

chitosan	F_A	$[\eta]$(mL/g)	$\bar{M}_w$	M_W (g/mol)	$\overline{DP}$
LMWc	0.55	300	90 000	200	450
HMWc	0.60	980	320 000	201	1592

[a]The fraction of acetylated units, (F_A), was determined by means of ^{1}H NMR. M_W stands for the molar mass of the repeating unit and was calculated on the basis of the chitosan chemical composition (Note: $GlcNH_2$·HCl was used for the calculation). Intrinsic viscosity, $[\eta]$, values were determined at 0.1 M NaCl, 20 mM AcOH/AcNa, pH 4.5, and T = 25 °C. The weight-average molecular mass, $\bar{M}_w$, was calculated in agreement with the Mark–Houwink–Sakurada equation, and $\overline{DP}$, that is, the average degree of polymerization, stands for the ratio between $\bar{M}_w$ and M_W of the chitosan repeating unit.

2.3. Assembly of Chitosan Gels at Neutral pH. 50 mg of hydrochloride chitosans were dissolved in 4 mL of deionized water. The pH was then adjusted to around 7.4 by adding aliquots of NaOH (0.1 M). 500 μL of 10× PBS and deionized water were added to obtain a final volume of 4.75 mL. Prior to rheological measurements, 250 μL of genipin dissolved in deionized water was mixed with chitosan solutions under magnetic stirring. The final pH and ionic

strength of the mixtures were ~7.4 and 168 mM, respectively, whereas the concentration of chitosan was 10 g/L, that is, 1% w/v, throughout all experiments. The final concentration of genipin was varied based on the desired glucosamine-to-genipin molar ratio, $R_{D/G}$, where D stands for the molar concentration of chitosan glucosamine and G for that of genipin. $R_{D/G}$ of 20, 40, or 90 was considered in this work, corresponding to a final genipin concentration of 1.04, 0.52, and 0.26 mM, respectively.[22]

2.4. Mechanical Investigation. Rheological measurements were performed using an HAAKE MARS III rheometer (Thermo Scientific), operating in oscillatory shear conditions. The experimental settings used to characterize chitosan gels were the following: titanium plates with 2° cone/plate geometry (Ø = 35 mm) and a gap of 0.105 mm. Upon the addition of genipin, the solutions were mixed under stirring for about 10 s and poured atop the plate. Mineral oil was used to seal the interface between the two plates in order to improve the thermal control and limit solvent evaporation. Time sweep experiments were carried out in strain-controlled conditions, with the strain, γ, of 3% kept constant throughout the experiment; frequency, ν, of 1 Hz; time of 7200 s; and T = 60 °C. The values of storage G' (elastic response) and loss G'' (viscous response) moduli were recorded as a function of time. After the time sweep, the mechanical spectra were recorded at T = 37 °C under oscillatory shear conditions, with the constant applied stress, τ, of 1 Pa (well within the linear viscoelasticity range) in the frequency range 0.01−100 Hz. At the end of frequency sweep measurements, stress sweep experiments were performed, with ν = 1 or 0.1 Hz, respectively, stress range $1 < \tau < 1000$ Pa, and T = 37 or 60 °C.

3. RESULTS AND DISCUSSION

Initially, a highly acetylated, low-molecular-weight chitosan (LMWc) was synthesized via heterogeneous deacetylation of chitin. The two-step low-temperature alkaline swelling/high-temperature deacetylation reaction enabled the controlled production of chitosan with a fraction of acetylated units, F_A, of 0.55, as determined by ^{1}H NMR, and low viscosity ($[\eta]$ = 300 mL/g). Chitosans with the fraction of acetylated units ranging from 0.4 to 0.6 are known to be well soluble at neutral pH without precipitation.[10,29] After solubilizing the highly acetylated chitosan at acidic pH and then raising and buffering it to 7.4, genipin was added, and the mixture was vigorously stirred prior to mechanical investigation. At acidic pH, highly deacetylated chitosans exhibit the majority of their glucosamine units in the protonated form, requiring an amount of genipin as high as 100 mM to promote gelation.[30−32] The use of highly acetylated chitosans, which are soluble at neutral pH, where the glucosamine units are deprotonated, allows the amount of cross-linker used for gelation to be drastically reduced.

To study the gelation progression of the system, time sweep analyses were performed on the mixtures with constant polymer concentration and variable glucosamine-to-genipin molar ratio, $R_{D/G}$. To improve reaction kinetics, the mixtures were cured at T = 60 °C.[22] Figure 1a shows gelling kinetics performed at $R_{D/G}$ = 20, as an example. The initial value of G' was slightly higher than G'', indicating that the early chain−chain cross-links caused mild reticulation at the beginning of incubation, prior to the development of a typical bluish color.[23] The values of the loss tangent, tan $\delta = G''/G'$, were also recorded as a function of time and are shown in Figure 1b tan δ decayed exponentially for all $R_{D/G}$ investigated, confirming the polymer network's transition from a viscous-like to a more elastic state. After ~4000 s, the loss tangents reached a plateau, indicating that the system completely gelled. At the end of the incubation period, all samples with different $R_{D/G}$ were positive

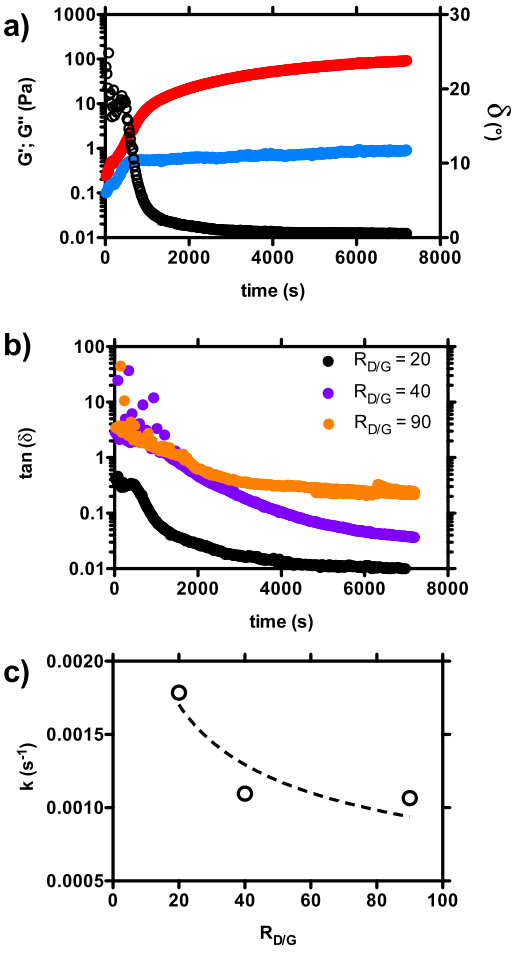

Figure 1. (a) Gelling kinetics of the chitosan−genipin system. G' (red dots), G'' (blue dots), and phase angle (δ) (black dots). (b) Time dependence of the loss tangent, tan δ (G''/G'), for networks showing different glucosamine-to-genipin molar ratio, $R_{D/G}$. (c) Dependence of the rate constant, k, on $R_{D/G}$; dashed line is drawn to guide the eye. Experimental conditions: [chitosan, LMWc] = 1% w/v, [genipin] = 0.26−1.04 mM; PBS as solvent, pH 7.4; gelling temperature, T = 60 °C.

to the inverted test tube (not reported), confirming the occurrence of gelation without exhibiting syneresis. Despite the fact that tan δ became nearly independent of time after 4000 s, a strong correlation emerged in the early stages of kinetics. Equation 4 was used to fit the experimental data

$$\tan\delta(t) = (\tan\delta_0 - \tan\delta_\infty)e^{-kt} + \tan\delta_\infty \quad (4)$$

where tan δ_0 is the value of the loss tangent at time zero, tan δ_∞ is the loss tangent at infinite time, and k is the rate constant.[33] For $R_{D/G} > 40$, the rate constant pointed to almost complete independence from network connectivity (Figure 1c).

In the control experiment, the time sweep performed on LMWc devoid of genipin revealed no significant variation in the rheological properties (Figure S1). It is worth noting, however, that the mechanical spectrum of LMWc showed a crossover point between G' and G'' at around 1 Hz (Figure S2). Although the values of G' and G'' remained nearly identical after the crossover frequency, the presence of chain entanglements can be tentatively hypothesized here (*vide infra*). It is worth noting that this result, which is comparable

to the one obtained with high-molecular-weight hyaluronan (M_w = 800,000),[34] is achieved with a low-molecular-weight polysaccharide.

The mechanical spectra of LMWc gels were then recorded. Regardless of the $R_{D/G}$ studied, the elastic modulus exceeded the viscous counterpart over at least two decades of frequencies (Figure 2). G' was almost frequency-independent

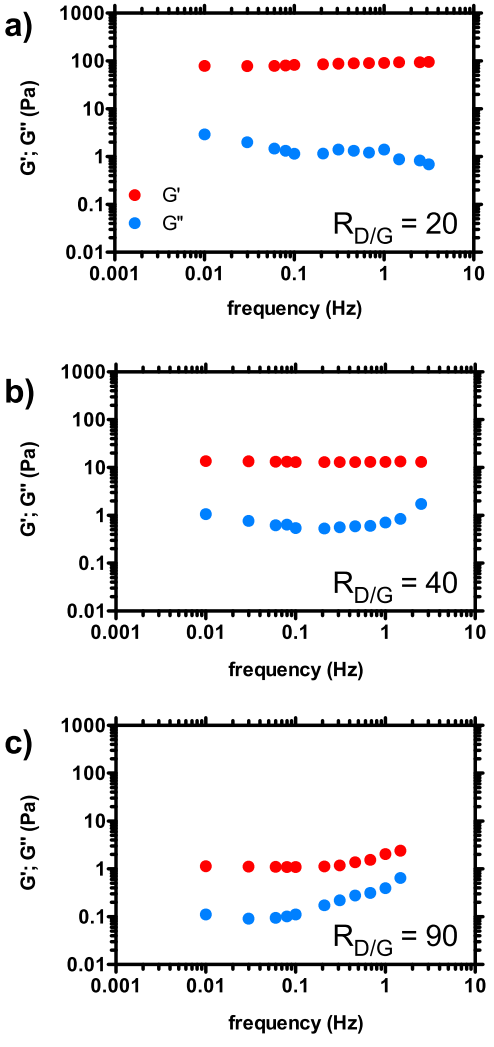

Figure 2. Frequency sweep on covalent chitosan–genipin gels. (a–c) Mechanical spectra of chitosan–genipin gels with different glucosamine-to-genipin molar ratio, $R_{D/G}$. G' (red dots) and G'' (blue dots). Experimental conditions: [chitosan, LMWc] = 1% w/v, [genipin] = 0.26–1.04 mM; PBS as solvent, and pH 7.4. After complete gelation was performed at T = 60 °C, all frequency sweep experiments were performed at T = 37 °C.

for ν < 0.1 Hz, indicating that chitosan gels behaved as strong elastic networks. For comparison, we calculated the elastic degree of chitosan gels at various $R_{D/G}$, with the G'/G'' ratio measured at ν = 0.1 Hz. The higher the network connectivity, the greater is the elastic degree of chitosan gels, with G'/G'' equal to 70, 20, and 10, for $R_{D/G}$ = 20, 40, and 90, respectively.

The frequency dependence of the elastic modulus exhibited by gels at different $R_{D/G}$ deserves an additional comment. While G' showed negligible frequency dependence in the high-connectivity regime ($R_{D/G} \leq 40$), an almost 2.5-fold increase in G' (approaching $G' \propto \nu^{0.6}$ at high enough frequencies) was observed for ν > 0.1 Hz in the case of $R_{D/G}$ = 90. Similar results were recently discovered for Matrigel, and they were linked to the material's positive effect on cell response.[35] This unusual behavior can be explained by the physical entanglements between the network's floppy and extended polysaccharide chains, as well as the non-reticulated LMWc (Figure S2). When the $R_{D/G}$ ratio is reduced to 40 or 20, the chitosan chains confined within the network are likely to be more stretched and fewer entanglements occur (not explored in the present work).

We conducted stress sweep experiments to learn more about the linear and nonlinear responses of chitosan gels. The linear stress–strain region was useful in determining the gel strength (Figure 3a). Curiously, the shear modulus of chitosan gels at

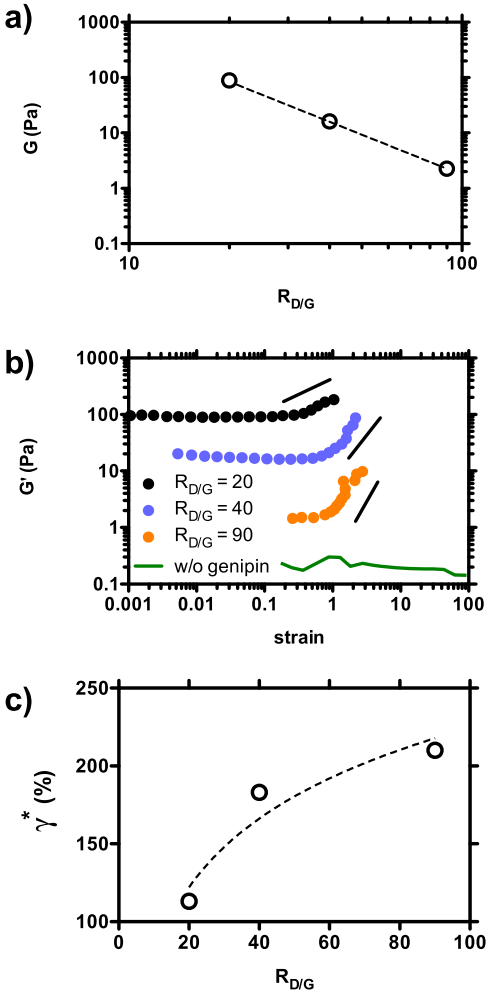

Figure 3. Low-connectivity covalent chitosan gels manifest adaptable strength and nonlinear elasticity. (a) Dependence of shear modulus, G, as a function of glucosamine-to-genipin molar ratio, $R_{D/G}$; dashed line is drawn to guide the eye. (b) Dependence of the elastic modulus, G', on the total strain applied for covalent chitosan gels with different $R_{D/G}$. Solid black lines are drawn to guide the eye on the strain hardening magnitude. Solid green line represents the dependence of elastic modulus for a chitosan solution devoid of genipin. (c) Dependence of the critical deformation at which the stiffening becomes dominant, γ^*, on $R_{D/G}$; dashed line is drawn to guide the eye. Experimental conditions: [chitosan, LMWc] = 1% w/v, [genipin] = 0.26–1.04 mM; PBS as solvent, and pH 7.4; after a complete gelation was performed at T = 60 °C, all stress sweep experiments were performed at T = 37 °C.

$R_{D/G}$ = 20 was nearly twice that of dual cross-link networks based on the lactose-modified chitosan (CTL) with the same glucosamine-to-genipin molar ratio (~90 *vs* 40 Pa), despite CTL having a higher molecular weight than chitosan.[22] Thus, the difference in the number of glucosamine units available to reticulate polysaccharide chains after genipin treatment results at the root of such a behavior, with F_D = 0.45 for chitosan and 0.21 for CTL, respectively.

The elastic moduli dependence on strain revealed a stiffening behavior at large deformations for all $R_{D/G}$ investigated, albeit exhibiting different magnitudes (Figure 3b). The phenomenon cannot be attributed to the polymer itself due to the lack of nonlinear hardening in samples deprived of genipin. Furthermore, contributions related to the chitosan's polyelectrolyte nature can be safely excluded[36] because it results almost uncharged at neutral pH, and our experimental conditions (pH and ionic strength) were kept constant throughout all experiments. As a result, we hypothesized that nonlinear elasticity could stem from the reorganization of the chitosan−genipin network while deforming.

Experimental points from stress *versus* strain curves were analyzed in terms of the Erk equation (eq 5) to elucidate the mechanism underlying strain hardening in chitosan gels

$$\tau = G_0 \gamma \, e^{(\gamma/\gamma^*)^2} \quad (5)$$

where τ is the applied stress, G_0 is the shear modulus at zero strain, γ is the experimental deformation, and γ^* is the critical strain at which the deviation from linearity becomes dominant.[37] Interestingly, we discovered a correlation between γ^* and $R_{D/G}$, clearly indicating that the onset of strain hardening can be shifted toward larger deformations while decreasing the genipin content (Figure 3c). According to MacKintosh and colleagues, strain hardening observed in collagen networks is related to fiber connectivity.[24] Similarly, Nonappa and colleagues discovered that the stiffening of semiflexible agarose fibrils was caused by low-connectivity networks.[3] In our case, chitosan is defined as a semiflexible worm-like chain, with the calculated persistence length, l_p, in the range 7−9 nm.[38,39] As a result, the addition of small amounts of genipin to chitosan promotes the formation of low-connectivity networks, similar to collagen or agarose gelling systems.

To determine the connectivity of chitosan gels at various $R_{D/G}$, the moles of elastically active chains per network unit volume were calculated using the rubber elasticity theory, as shown below (eq 6)

$$\rho = \frac{G}{RT} \quad (6)$$

where ρ represents the density of elastically active chains (mol/m^3), G is the shear modulus, R is the universal gas constant, and T is the absolute temperature. While correlating γ^* as a function of cross-linking density, an intriguing scenario emerged (Figure 4). The experimental points define a threshold, identifying two areas of interest: (i) low connectivity, which causes delayed onset of strain hardening and (ii) high connectivity, which promotes early onset of stiffening. Despite the fact that chitosan is semiflexible rather than rod-like, the dependence of critical strain on connectivity followed a power-law behavior, with $\gamma^* \propto \rho^{-0.17}$, where n exponent was comparable with that found in the collagen matrix.[24]

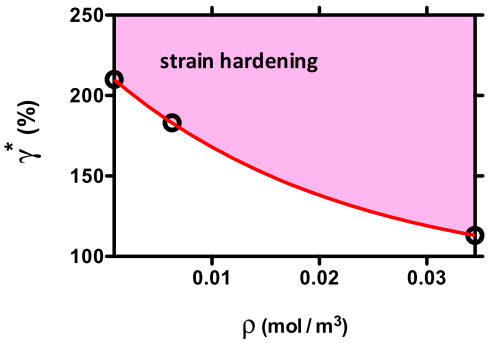

Figure 4. Dependence of the critical deformation at which the strain hardening becomes dominant, γ^*, on the moles of elastically active chitosan chains per network unit volume, ρ, upon varying network connectivity, that is, $R_{D/G}$; solid red line defines linear from nonlinear elasticity regions. Experimental conditions: [chitosan, LMWc] = 1% w/v, [genipin] = 0.26−1.04 mM; PBS as solvent, and pH 7.4.

As previously predicted, the strain hardening phenomenon in the chitosan−genipin system could then result from the temporary physical entanglements among the polymer chains that comprise the network. To test our hypothesis, we synthesized a HMWc with a similar acetylation degree (*i.e.*, F_A = 0.60) by homogeneous re-*N*-acetylation of a template, with starting F_A = 0.14. Following that, we assembled chitosan gels with the same polymer concentration, that is, 1% w/v, but different $R_{D/G}$, namely 20 (high connectivity) or 90 (low connectivity). When high-molecular-weight chitosan gels with $R_{D/G}$ = 20 were studied, a crack-type fracture rather than strain hardening was detected (Figure 5). When the amount of genipin was reduced, strain hardening reappeared. When the effect of the elastic modulus was compared at T = 37 and 60 °C (Figure S3), an increase in the elastic response was observed for the former. In the latter case, however, the relative increase of G' in the nonlinear regime was more pronounced. Preliminary research was also conducted on the effect of frequency on oscillatory stimulation (Figure S4). When the

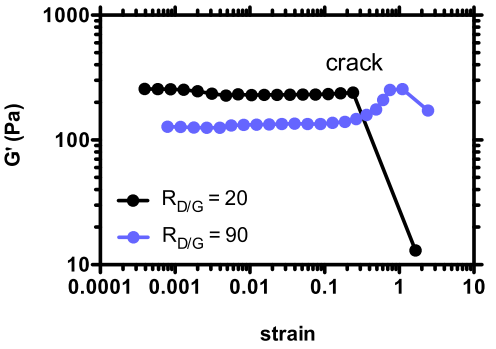

Figure 5. Network connectivity influences covalent chitosan gel performance at large deformations, eliciting crack-type fracture or nonlinear elasticity. The plot reports the dependence of the elastic modulus (G') on the total strain applied for chitosan−genipin gels assembled *via* high-molecular-weight chitosan, with $R_{D/G}$ = 20 (black) and and $R_{D/G}$ = 90 (purple). Experimental conditions: [chitosan, HMWc] = 1% w/v; [genipin] = 1.04 or 0.26 mM; PBS as solvent, and pH 7.4; after complete gelation was performed at T = 60 °C, all stress sweep experiments were performed at T = 37 °C.

frequency was reduced from 1 to 0.1 Hz, γ^* increased from 210 to 280% for LMWc-based gels at $R_{D/G}$ = 90, indicating that the engagement of entanglements requires higher strain values to elicit the same effect when the stress is applied at a lower angular velocity. Collectively, these findings point to the importance of temporary (and weak) physical entanglements formed by semiflexible chitosan chains in determining nonlinear strain hardening in conjunction with the overall network connectivity.

To propose a model for the current chitosan–genipin gelling system, we consider the molecular offset of the strain hardening as a result of temporary cross-links formed by polysaccharide chains when the critical strain is exceeded. While they are most likely present in the gel network at rest, their contribution is negligible due to the rapid (mutual) disentanglement of the semiflexible chitosan chains. For semiflexible chains with permanent genipin-type cross-links, the rate of entanglement equals the rate of disentanglement at low strain. As the shear strain increases, the chains are forcedly packed. When the strain exceeds γ^*, the entanglement rate exceeds the disentanglement one. This is expected to result in strain hardening (Scheme 1). The current model accounts for the chemical or physical nature of temporary cross-links with no loss of generality.

Scheme 1. Scheme Depicting the Formation of Temporary Entanglements in Covalent Chitosan Gels[a]

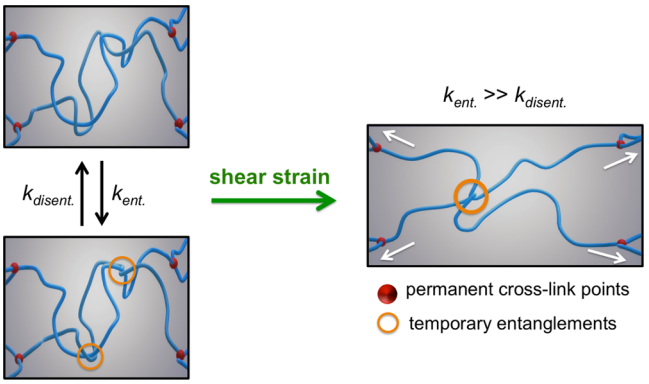

[a]At rest, low-connectivity networks are composed of chitosan chains stabilized by permanent genipin-type cross-link points. In parallel, transient entanglements originate from the semiflexible chitosan chains. Here, the rate of entanglement (k_{ent}) equals the rate of disentanglement (k_{disent}). Upon application of shear strain, chitosan chains are forced to approach each other, causing $k_{ent} \gg k_{disent}$. Therefore, the reinforcement of physical entanglements takes place, which is responsible for the onset of nonlinear elasticity (strain hardening).

We attempted to calculate the contour length (L_c) of chitosan chains between two cross-link points within the realm of the description of the chitosan–genipin gelling system as the model (see Appendix in the Supporting Information for further details). Table S1 shows that, as the network connectivity is reduced, L_c increases progressively. It is reasonable to conclude that the shorter the contour length of the polymer chain between the cross-link points, the fewer are the physical interchain entanglements that could be formed when the stress is applied. When the connectivity is reduced, the contour length of the chitosan chain between the cross-link points expands, increasing the likelihood of interchain physical entanglements, which are responsible for the onset of strain hardening. As a result, strain hardening is determined by the unbalancing of entangling–disentangling of chains between permanent cross-links, which is influenced by their packing and stretching in turn. When the connectivity is set high ($R_{D/G}$ = 20 in LMWc-based gels), a limited strain extends the partially stretched chains between the cross-link points, favoring entangling over disentangling of the few intertwined chains and resulting in the engagement of temporary physical cross-links. Given higher L_c, greater intertwining of chains between cross-links is expected in LMWc-based gels at $R_{D/G}$ = 90. In these circumstances, a superior stretching of the network is required to overcome the flexibility of the chains between permanent cross-link points, thereby favoring entanglements over disentanglements. In contrast, strain hardening was not observed in HMWc-based gels at $R_{D/G}$ = 20. The higher connectivity, as reflected by the higher shear modulus, results in quite extended chitosan chains between the genipin-type cross-links already at rest, and intertwining (and hence entangling) does not occur at all. It is unknown how the chemical composition of chitosan affects strain hardening. Because this effect was never observed in highly deacetylated chitosan samples, it is reasonable to conclude that the reduction of glucosamine units, and the resulting lower (positive) charge on the polysaccharide, contributes to the nonlinear elasticity.

When these factors are considered together, it is tempting to propose a relationship between the calculated contour length of chitosan chains between permanent cross-link points and the macroscopic response of related gels to mechanical stimulation. Figure 6 depicts the relationship between the inverse of the number of Khun's segments in the contour length and the relative variation of the elastic modulus, G'_{rel} (eq 7)

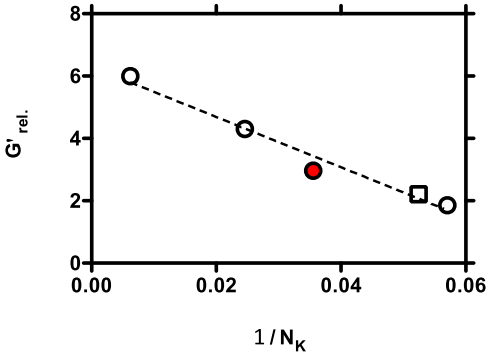

Figure 6. Strain hardening depends on the number of Khun's segments in the contour length of chitosan chain between two permanent cross-link points. The plot reports the dependence of the relative variation of the elastic modulus (G'_{rel}, eq 7 in the main text) on the inverse of Khun's segments in the contour length of the chitosan chain between two permanent cross-link points, $1/N_K$, for chitosan gels at different experimental conditions investigated in this study. The red dot represents the case of stress sweep experiment recorded at T = 60 °C, whereas the squared one is that of HMWc with $R_{D/G}$ = 90. The dotted line represents the linear best fit of experimental data (R^2 = 0.97).

$$G'_{rel} = \frac{G'_{max}}{G'_{\tau 0}} \quad (7)$$

where G'_{max} is the highest value reached by the elastic modulus in the stress sweep experiments, and $G'_{\tau 0}$ is the value derived from the Soskey–Winter model in the low stress regime.[27] While the current relationship is intended to be purely phenomenological, a linear correlation was discovered. As a result, the more extended and flexible the chain between permanent cross-link points in the gel network, the greater is the number of chain entanglements that overcomes the disentanglements upon stretching. It is now possible to use the G'_{rel} *vs* $1/N_K$ correlation to calculate the smallest number of Khun's segments that contributes to strain hardening. The unitary value of G'_{rel} corresponding to $N_K = 15$ is determined by the linear best fit of experimental data.

4. CONCLUSIONS

To summarize, we sought to define the unusual strain hardening behavior of covalent chitosan gels at neutral pH. While it is well known that viscoelastic chitosan gels exhibit strain softening or, worse, dramatically fracture under critical experimental shearing conditions, we show here that chitosan gels assembled at neutral pH and physiological osmolarity can exhibit nonlinear elasticity, or strain hardening, if the initial network connectivity is set low. An unbalance of entanglement over disentanglement among semiflexible chitosan chains is identified here at the root of nonlinear elasticity, which results from the engagement of temporary physical cross-links. When connectivity is low, this effect is caused by the length and flexibility of the chitosan chain between permanent cross-links. Despite being developed for the case of highly acetylated chitosans, the current model may have general applicability in describing loosely reticulated networks of semiflexible polymers prone to interchain entanglements. Our results could also explain the contradictory findings in gelling systems based on chitosan derivatives. For example, while crack-type fracture in catechol-modified chitosan gels may now be associated with high connectivity and whole entanglement ([genipin] ∼ 3 mM, C_p = 1.5% w/v),[20] strain hardening in PEG-grafted chitosan gels may be associated with low connectivity and moderate entanglement ([genipin] = 0.5 mM, C_p = 1.3% w/v).[21] Furthermore, we found a correlation between critical strain, which marks the onset of nonlinear elasticity, and network connectivity, being $\gamma^* \propto \rho^n$, where the exponent n is close to that calculated for the collagen matrix (0.17 *vs* 0.14).[24] Thus, our findings pave the way to new ideas about the use of neutral pH-soluble chitosans in assembling extracellular matrix mimics endowed with tunable biodegradability,[1,40] with potential applications in the tissue engineering sector.

■ ASSOCIATED CONTENT

Supporting Information

The Supporting Information is available free of charge at https://pubs.acs.org/doi/10.1021/acs.biomac.1c00293.

Calculation of the contour length of chitosan chains between the cross-link points for the chitosan–genipin gelling system; additional figures. (PDF)

■ AUTHOR INFORMATION

Corresponding Author

Pasquale Sacco − *Department of Life Sciences, University of Trieste, Trieste I-34127, Italy;* orcid.org/0000-0002-4483-5099; Phone: +39-040-5588733; Email: psacco@units.it

Authors

Franco Furlani − *Department of Life Sciences, University of Trieste, Trieste I-34127, Italy;* Present Address: Present address: Institute of Science and Technology for Ceramic, National Research Council, Via Granarolo 64, I-48018 Faenza, Italy; orcid.org/0000-0001-5986-1727

Andrea Marfoglia − *Department of Life Sciences, University of Trieste, Trieste I-34127, Italy*

Eleonora Marsich − *Department of Medicine, Surgery and Health Sciences, University of Trieste, Trieste I-34129, Italy*

Ivan Donati − *Department of Life Sciences, University of Trieste, Trieste I-34127, Italy;* orcid.org/0000-0003-3752-8346

Complete contact information is available at: https://pubs.acs.org/10.1021/acs.biomac.1c00293

Author Contributions

#F.F. and A.M contributed equally to this manuscript. The manuscript was written through contributions of all authors. Data curation and designation of experiments: I.D. and P.S. Investigation: F.F., A.M., and E.M. Methodology, F.F., A.M., E.M., I.D., and P.S. Writing original draft: F.F. and A.M. Writing final draft: I.D., P.S.

Notes

The authors declare no competing financial interest.

■ ACKNOWLEDGMENTS

This study was supported by the INTERREG V-A ITALIA-SLOVENIA 2014–2020 BANDO 1/2016 ASSE 1–project BioApp 1472551605 granted to I.D.

■ REFERENCES

(1) Storm, C.; Pastore, J. J.; MacKintosh, F. C.; Lubensky, T. C.; Janmey, P. A. Nonlinear elasticity in biological gels. *Nature* **2005**, *435*, 191–194.

(2) Hashemnejad, S. M.; Kundu, S. Rheological properties and failure of alginate hydrogels with ionic and covalent crosslinks. *Soft Matter* **2019**, *15*, 7852–7862.

(3) Bertula, K.; Martikainen, L.; Munne, P.; Hietala, S.; Klefström, J.; Ikkala, O.; Nonappa. Strain-Stiffening of Agarose Gels. *ACS Macro Lett.* **2019**, *8*, 670–675.

(4) Schuster, E.; Lundin, L.; Williams, M. A. K. Investigating the Relationship between Network Mechanics and Single-Chain Extension Using Biomimetic Polysaccharide Gels. *Macromolecules* **2012**, *45*, 4863–4869.

(5) McAllister, J. W.; Lott, J. R.; Schmidt, P. W.; Sammler, R. L.; Bates, F. S.; Lodge, T. P. Linear and Nonlinear Rheological Behavior of Fibrillar Methylcellulose Hydrogels. *ACS Macro Lett.* **2015**, *4*, 538–542.

(6) Das, R. K.; Gocheva, V.; Hammink, R.; Zouani, O. F.; Rowan, A. E. Stress-stiffening-mediated stem-cell commitment switch in soft responsive hydrogels. *Nat. Mater.* **2016**, *15*, 318–325.

(7) Guimarães, C. F.; Gasperini, L.; Marques, A. P.; Reis, R. L. The stiffness of living tissues and its implications for tissue engineering. *Nat. Rev. Mater.* **2020**, *5*, 351–370.

(8) Vårum, K. M.; Antohonsen, M. W.; Grasdalen, H.; Smidsrød, O. Determination of the degree of N-acetylation and the distribution of N-acetyl groups in partially N-deacetylated chitins (chitosans) by high-field n.m.r. spectroscopy. *Carbohydr. Res.* **1991**, *211*, 17–23.

(9) Sacco, P.; Furlani, F.; de Marzo, G.; Marsich, E.; Paoletti, S.; Donati, I. Concepts for Developing Physical Gels of Chitosan and of Chitosan Derivatives. *Gels* **2018**, *4*, 67.

(10) Vårum, K. M.; Ottøy, M. H.; Smidsrød, O. Water-solubility of partially N-acetylated chitosans as a function of pH: effect of chemical composition and depolymerisation. *Carbohydr. Polym.* **1994**, *25*, 65−70.
(11) Montembault, A.; Viton, C.; Domard, A. Physico-chemical studies of the gelation of chitosan in a hydroalcoholic medium. *Biomaterials* **2005**, *26*, 933−943.
(12) Boucard, N.; Viton, C.; Domard, A. New Aspects of the Formation of Physical Hydrogels of Chitosan in a Hydroalcoholic Medium. *Biomacromolecules* **2005**, *6*, 3227−3237.
(13) Montembault, A.; Viton, C.; Domard, A. Rheometric Study of the Gelation of Chitosan in Aqueous Solution without Cross-Linking Agent. *Biomacromolecules* **2005**, *6*, 653−662.
(14) Sacco, P.; Borgogna, M.; Travan, A.; Marsich, E.; Paoletti, S.; Asaro, F.; Grassi, M.; Donati, I. Polysaccharide-Based Networks from Homogeneous Chitosan-Tripolyphosphate Hydrogels: Synthesis and Characterization. *Biomacromolecules* **2014**, *15*, 3396−3405.
(15) Sacco, P.; Paoletti, S.; Cok, M.; Asaro, F.; Abrami, M.; Grassi, M.; Donati, I. Insight into the ionotropic gelation of chitosan using tripolyphosphate and pyrophosphate as cross-linkers. *Int. J. Biol. Macromol.* **2016**, *92*, 476−483.
(16) Khong, T. T.; Aarstad, O. A.; Skjåk-Bræk, G.; Draget, K. I.; Vårum, K. M. Gelling concept combining chitosan and alginate-proof of principle. *Biomacromolecules* **2013**, *14*, 2765−2771.
(17) Martínez-Martínez, M.; Rodríguez-Berna, G.; Gonzalez-Alvarez, I.; Hernández, M. J.; Corma, A.; Bermejo, M.; Merino, V.; Gonzalez-Alvarez, M. Ionic Hydrogel Based on Chitosan Cross-Linked with 6-Phosphogluconic Trisodium Salt as a Drug Delivery System. *Biomacromolecules* **2018**, *19*, 1294−1304.
(18) Heimbuck, A. M.; Priddy-Arrington, T. R.; Padgett, M. L.; Llamas, C. B.; Barnett, H. H.; Bunnell, B. A.; Caldorera-Moore, M. E. Development of Responsive Chitosan−Genipin Hydrogels for the Treatment of Wounds. *ACS Appl. Bio Mater.* **2019**, *2*, 2879−2888.
(19) Dimida, S.; Demitri, C.; De Benedictis, V. M.; Scalera, F.; Gervaso, F.; Sannino, A. Genipin-cross-linked chitosan-based hydrogels: Reaction kinetics and structure-related characteristics. *J. Appl. Polym. Sci.* **2015**, *132*, 42256.
(20) Xu, J.; Strandman, S.; Zhu, J. X. X.; Barralet, J.; Cerruti, M. Genipin-crosslinked catechol-chitosan mucoadhesive hydrogels for buccal drug delivery. *Biomaterials* **2015**, *37*, 395−404.
(21) Chang, F.-C.; Levengood, S. L.; Cho, N.; Chen, L.; Wang, E.; Yu, J. S.; Zhang, M. Crosslinked Chitosan-PEG Hydrogel for Culture of Human Glioblastoma Cell Spheroids and Drug Screening. *Adv. Ther.* **2018**, *1*, 1800058.
(22) Sacco, P.; Furlani, F.; Marfoglia, A.; Cok, M.; Pizzolitto, C.; Marsich, E.; Donati, I. Temporary/Permanent Dual Cross-Link Gels Formed of a Bioactive Lactose-Modified Chitosan. *Macromol. Biosci.* **2020**, *20*, 2000236.
(23) Pizzolitto, C.; Cok, M.; Asaro, F.; Scognamiglio, F.; Marsich, E.; Lopez, F.; Donati, I.; Sacco, P. On the Mechanism of Genipin Binding to Primary Amines in Lactose-Modified Chitosan at Neutral pH. *Int. J. Mol. Sci.* **2020**, *21*, 6831.
(24) Sharma, A.; Licup, A. J.; Jansen, K. A.; Rens, R.; Sheinman, M.; Koenderink, G. H.; MacKintosh, F. C. Strain-controlled criticality governs the nonlinear mechanics of fibre networks. *Nat. Phys.* **2016**, *12*, 584−587.
(25) Sacco, P.; Baj, G.; Asaro, F.; Marsich, E.; Donati, I. Substrate Dissipation Energy Regulates Cell Adhesion and Spreading. *Adv. Funct. Mater.* **2020**, *30*, 2001977.
(26) Varum, K. M.; Smidsrød, O.; Mustaparta, E. J. Chitosan preparation. WO 2003,011,912 A1.
(27) Sacco, P.; Cok, M.; Asaro, F.; Paoletti, S.; Donati, I. The role played by the molecular weight and acetylation degree in modulating the stiffness and elasticity of chitosan gels. *Carbohydr. Polym.* **2018**, *196*, 405−413.
(28) Berth, G.; Dautzenberg, H. The degree of acetylation of chitosans and its effect on the chain conformation in aqueous solution. *Carbohydr. Polym.* **2002**, *47*, 39−51.
(29) Sannan, T.; Kurita, K.; Iwakura, Y. Studies on chitin, 2. Effect of deacetylation on solubility. *Makromol. Chem. Macromol. Symp.* **1976**, *177*, 3589−3600.
(30) Barbosa, J. S.; Ribeiro, A.; Testera, A. M.; Alonso, M.; Arias, F. J.; Rodríguez-Cabello, J. C.; Mano, J. F. Development of biomimetic chitosan-based hydrogels using an elastin-like polymer. *Adv. Eng. Mater.* **2010**, *12*, B37−B44.
(31) Bi, L.; Cao, Z.; Hu, Y.; Song, Y.; Yu, L.; Yang, B.; Mu, J.; Huang, Z.; Han, Y. Effects of different cross-linking conditions on the properties of genipin-cross-linked chitosan/collagen scaffolds for cartilage tissue engineering. *J. Mater. Sci. Mater. Med.* **2011**, *22*, 51−62.
(32) Mi, F.-L.; Sung, H.-W.; Shyu, S.-S.; Su, C.-C.; Peng, C.-K. Synthesis and characterization of biodegradable TPP/genipin co-crosslinked chitosan gel beads. *Polymer* **2003**, *44*, 6521−6530.
(33) Sacco, P.; Furlani, F.; Paoletti, S.; Donati, I. pH-Assisted Gelation of Lactose-Modified Chitosan. *Biomacromolecules* **2019**, *20*, 3070−3075.
(34) Travan, A.; Fiorentino, S.; Grassi, M.; Borgogna, M.; Marsich, E.; Paoletti, S.; Donati, I. Rheology of mixed alginate-hyaluronan aqueous solutions. *Int. J. Biol. Macromol.* **2015**, *78*, 363−369.
(35) Moreno-Manzano, V.; Zaytseva-Zotova, D.; López-Mocholí, E.; Briz-Redón, Á.; Løkensgard Strand, B.; Serrano-Aroca, Á. Injectable Gel Form of a Decellularized Bladder Induces Adipose-Derived Stem Cell Differentiation into Smooth Muscle Cells In Vitro. *Int. J. Mol. Sci.* **2020**, *21*, 8608.
(36) Han, B.; Chery, D. R.; Yin, J.; Lu, X. L.; Lee, D.; Han, L. Nanomechanics of layer-by-layer polyelectrolyte complexes: a manifestation of ionic cross-links and fixed charges. *Soft Matter* **2016**, *12*, 1158−1169.
(37) Erk, K. A.; Henderson, K. J.; Shull, K. R. Strain Stiffening in Synthetic and Biopolymer Networks. *Biomacromolecules* **2010**, *11*, 1358−1363.
(38) Cok, M.; Viola, M.; Vecchies, F.; Sacco, P.; Furlani, F.; Marsich, E.; Donati, I. N-isopropyl chitosan. A pH- and thermo-responsive polysaccharide for gel formation. *Carbohydr. Polym.* **2020**, *230*, 115641.
(39) Christensen, B. E.; Vold, I. M. N.; Vårum, K. M. Chain stiffness and extension of chitosans and periodate oxidised chitosans studied by size-exclusion chromatography combined with light scattering and viscosity detectors. *Carbohydr. Polym.* **2008**, *74*, 559−565.
(40) Nordtveit, R. J.; Vårum, K. M.; Smidsrød, O. Degradation of fully water-soluble, partially N-acetylated chitosans with lysozyme. *Carbohydr. Polym.* **1994**, *23*, 253−260.